Non-Gaussian Wind Pressure Characteristics of HAWT Tower System with and Without Rotor

N. I. Haroon Rashid[1†], S. Nadaraja Pillai[2], S. Selvi Rajan[3] and C. Senthil Kumar[1]

[1]*Department of Aerospace Engineering, Madras Institute of Technology, Anna University, Tamil Nadu, India*
[2]*School of Mechanical Engineering, SASTRA University, Tamil Nadu, India*
[3]*Structural Engineering Research Centre, CSIR, Taramani, Chennai, Tamil Nadu, India*

†*Corresponding Author Email: aeroharoonrashid@gmail.com*

ABSTRACT

Generally, the Gaussian assumption has been considered in analyzing the data pertaining to the wind effects on the structures or bluff bodies due to the abundance of the statistical information. In this study, Horizontal Axis Wind Turbine (HAWT) tower system with dimension of 1:330 scale is studied in order to understand their peak pressure behavior for wind resistant design. Generally, tower systems are constructed of various geometrical structures such as lattice towers, tubular steel towers, concrete towers, but in this present study tubular cylindrical tower is only considered. Simultaneous pressure measurements on the surface of the tower were performed in the low-speed boundary layer wind tunnel with test section dimension of 18 m × 2.5 m × 2.15 m having Reynolds number ranging from 10^2 to 10^4. The peak pressures acting on the tower systems are calculated for a number of ten-minute samples on various locations of the wind turbine. Peak value calculations based on Gaussian and Non – Gaussian processes are discussed mathematically and applied to the data collected from the wind tunnel tests. A mathematical model of Davenport and Kareem – Zhou is used in calculating the peak factor for Gaussian and non – Gaussian processes, respectively. The results indicate that higher moments dominate as most of the distribution is skewed and with kurtosis value. Henceforth, a study on extreme value analysis is deemed necessary in designing wind resistant structures or bluff bodies. Considering Gaussian nature alone may under-represent the peak value of the HAWT tower.

Keywords: Probability distribution; Tower system; Peak factor; HAWT; Non-Gaussian.

NOMENCLATURE

g	peak factor		process
g_b	peak factor for any bandwidth	v_{ng}	mean crossing rate for non-Gaussian
g_{ng}	non-Gaussian peak factor		process
H_n	Hermite moment of order n.		
m_0, m_2, m_4	spectral moments	ε	bandwidth parameter
$S(n)$	power spectrum	ζ_3	skewness of the random distribution
v_g	mean crossing rate for Gaussian	ζ_4	kurtosis of the random distribution

1. INTRODUCTION

The attention on wind energy resources has been increasing in the recent years due to depletion of fossil fuels, negative environmental impact and a plethora of innovative technological solutions. Horizontal axis wind turbine (HAWT) is a known technology to harness electrical energy by converting the kinetic energy of wind into mechanical and then into electrical energy. World wind energy (2014) reports that, total wind energy capacity of the world reaches 369 GW, out of which 50 MW added in 2014 itself, and also the cumulative market growth of 16%. Various configurations of the wind turbine tower have been built around the world; however, tubular tower configuration is preferred over lattice towers. This is because the area occupied is smaller and the distance between rotor and tower is increased to reduce the aerodynamic interference. Otherwise, from a structural point of view, the tubular tower is a statically determinate structure, such structures reported easier failure than common

structures as outlined in Chien *et al.* (2009). During the last decade, several wind turbine towers are damaged due to strong wind conditions. Wind turbine tower damage due to strong wind on the Miyakojima Island in Japan is reported by Tamura. (2009). Extreme value pressure distribution is not only important in many high rise structures, but also in wind turbine tower systems. Also, the tubular tower structures are designed as truncated cones with the change in diameter, which is increasing towards the base in order to increase the strength and to decrease the materials involved. Lavassas *et al.* (2003) demonstrated that the steel tubular tower has a high aspect ratio that makes it particularly more slender and wind sensitive than any other structure. The numerical investigation had been performed on stiffened and unstiffened shells by Dimopoulos *et al.* (2012) and the result delineates that the slender shell structure has the tendency to greatly resist buckling in the elastic region. The structural analysis of steel towers has been studied in order to ensure the safe design, however, the nature of the pressure distribution around the tower contributes remarkably. Total mean wind forces and local peak pressures are measured and discussed for the wind turbine nacelle systems with various wind directions and the importance of peak wind forces and peak wind pressure distribution on the wind turbine nacelle is studied by Noda *et al.* (2005). Pillai *et al.* (2009) discussed the peak factor for the general random processes in wind engineering. Gusella *et al.* (2000) studied the non-Gaussian characteristics in both time and frequency domain which can be considered for such surface pressure of HAWT. There are various reasons reported for such wind turbine tower out of which non-gaussianity of the HAWT cannot be neglected. Non-Gaussian response characteristics in a wind turbine tower have been discussed by Binh *et al.* (2008), where the non-gaussianity in the HAWT is dominant. However, the basic study of the wind pressure characteristics may be an important challenge while the rotor is rotating.

Kwon *et al.* (2012) compared the wind loading effects on wind turbine power systems due to normal boundary layer wind and at gust front loading conditions. The non-Gaussian random process analysis is inevitable for statistical prediction of any random process where nonlinear characteristics are present. Davenport's (1964) paper on peak factor still followed in many international standards based on Gaussian processes and application to gust loading has certain limitations in considering non-Gaussian probability density function. Cartwright and Longuet-Higgins (1956) discussed statistical maxima and minima for the random processes by considering the narrow band or wide band in the frequency domain, where non- gaussianity is not considered.

The probability density functions which are applicable for representing non-Gaussian processes have been reported (Pillai *et al.* 2009; Gurley *et al.* 1997; Kareem *et al.* 2004; Grigoroiu. 1984 and Winterstein. 1985). In the present study, for the non-Gaussian probability distribution, Gram- Charlier probability density function based on the Hermite polynomial is used. For the simplicity and the physical significance up to the fourth moment of the Hermite polynomials are outlined in Kareem *et al.* (2004)

Although considerable attention has been given to the random process in the HAWT tower, comparatively little is known of non-Gaussian analysis and the associated probabilistic prediction of the process in wind turbine tower systems is necessary. In this study, simultaneous pressure measurement around the wind turbine tower with and without rotor for various Reynolds number is made in the low-speed wind tunnel and peak pressures were measured. From this data, the calculated peak factor is compared with various peak factors such as Davenport's peak factor, Cartwright – Longuet Higgins peak factor and Kareem – Zhou's peak factor.

2. PEAK FACTOR

In engineering design of wind turbine tower systems, it is important to determine the expected maximum value due to the stochastic nature of the processes. The expected maximum value for any random process $X(t)$ can be represented by Davenport (1964) as

$$\overline{X}_{max} = \overline{X} + g.\sigma_x \tag{2.1}$$

Here $\overline{X}_{max}$ is the expected maximum value, $\overline{X}$ is the mean value, g is the peak factor and σ_x is the standard deviation of the random processes. In general, the available procedures are reasonably well established to predict the peak factor g for the Gaussian process, but they are less clear for the non-Gaussian process in the random analysis. In this section, the derivation for calculating the maximum of any non-Gaussian random process is derived. The probability density functions which are applicable for representing non-Gaussian processes have been reported (Pillai *et al.* 2009; Kareem *et al.* 2004 and Winterstein. 1985). In this study, the Gram- Charlier probability density function based on the Hermite polynomial is discussed. Also, the derived probability density function characterizes the non-Gaussian parameters like Skewness and kurtosis.

2.1 Probability Density Distribution of Gaussian Process

Consider a stationary random process having normal probability distribution with mean m_x and standard deviation σ_x. The reduced variate is defined as $x_0(t) = [x - m_x]/\sigma_x$. The probability density function can be written as

$$P(x_0) = \frac{1}{\sqrt{2\pi}} \exp\left(-\frac{1}{2}x_0^2\right) \tag{2.2}$$

The cumulative probability density function, $Q(x_0)$

, will be defined as the probability of the function exceeding some value x_0.

$$Q(x_0) = \frac{1}{\sqrt{2\pi}} \left[\begin{array}{l} \int_{x_0}^{\infty} \exp(-\frac{1}{2}x^2)dx + (\sqrt{1-\varepsilon^2}) \\ \\ \exp(-\frac{1}{2}x_0^2) \int_{-\infty}^{x_0\left(\sqrt{1-\varepsilon^2}/\varepsilon\right)} \exp(-\frac{1}{2}x^2)dx \end{array} \right]$$

(2.3)

In which

$$\varepsilon = \left(\sqrt{1 - \left(\frac{m_2^2}{m_0 m_4} \right)} \right)$$

(2.4)

Where,

$$m_r = \int_0^{\infty} n^r S(n)dn$$

(2.5)

$S(n)$ is the power spectrum of the random function at the frequency n. For narrowband spectrum $\varepsilon = 0$ and it increases as the bandwidth increases, reaches $\varepsilon = 1$ for the wideband processes.

2.2 Davenport's Peak factor formula

Let us consider the sample of N maxima, the probability $P_{\max}(x_0)$ the largest of them has the value, is the probability that one of the maxima has his value and the rest are smaller, that can be written as follows

$$P_{\max}(x_0) = N\left[1 - Q(x_0)\right]^{N-1} P(x_0)$$

(2.6)

$$Q(x_0) = \xi / N$$

(2.7)

Where, $0 \le \xi \le N$. For large values of N, it can be written by considering limit in the asymptotic form as

$$P_{\max}(x_0)dx_0 = d\left[1 - \xi / N\right]^{N-1} = d\exp(-NQ(x_0))$$

(2.8)

Here, considering the (bandwidth parameter ε which is negligible and assumed that it is a narrow band process. Also, in this present study, only the non-gaussianity and whether it is narrowband or broadband in the frequency domain is not considered in the evaluation of peak factor.

$$Q(x_0) \cong \left\{ \begin{array}{l} (\sqrt{1-\varepsilon^2})\exp(-\frac{1}{2}x_0^2) + \\ \\ terms\ of\ higher\ order\ \frac{1}{x_0^3}\exp\left[-\frac{1}{2}\left(\frac{x_0^2}{\varepsilon^2}\right)\right] \end{array} \right\}$$

(2.9)

For the maxima, during the period N can be represented as,

$$N = \nu T = \left(\frac{m_4}{m_2} \right)^{1/2} T$$

(2.10)

Where T is the time period. From Eqs. (2.7), (2.9) it can be written as

$$\xi = NQ(\eta) = \nu T \exp\left(-\frac{1}{2}x_0^2 \right)$$

(2.11)

The probability density of the largest of the maxima is given by

$$P_{\max}(x_0)dx_0 = d\exp\left[-\nu T \exp\left(-\frac{1}{2}x_0^2 \right) \right]$$
$$= \exp(-\xi)d\xi$$

(2.12)

The mean of the maximum value can be represented as

$$\bar{x}_{0\max} = \int_{-\infty}^{\infty} x_0 P_{\max}(x_0)dx_0$$
$$= \int_{-\infty}^{\infty} x_0 \exp(-\xi)d\xi$$

(2.13)

Then the value of the $\bar{x}_{0\max}$ can be calculated as shown in the Eq. (2.14)

$$\bar{x}_{0\max} = \sqrt{\left((2\log \nu T) - 2\log_e \xi \right)}$$
$$= \sqrt{(2\log \nu T)} - \left(\frac{\log \xi}{\sqrt{2\log \nu T}} \right) - \frac{1}{2}\frac{\log^2 \xi}{\sqrt{(2\log \nu T)^3}} + ...$$

(2.14)

Using the expression for $\bar{x}_{0\max}$, the Eq. (2.13) can be evaluated using some standard integrals found in the extreme value analysis, namely

$$\int_0^{\infty} \log_e \xi \exp(-\xi)d\xi = -\gamma$$

(2.15)

Where $\gamma = 0.5772$, the above Eq. (2.14) can be approximated and can be shown as

$$\bar{x}_{0\max} \approx \left\{ \left[2\log N\right]^{1/2} + \gamma\left[2\log N\right]^{-1/2} \right\}$$

$$g \approx \left\{ \left[2\log N\right]^{1/2} + \frac{\gamma}{\left[2\log N\right]^{-1/2}} \right\}$$

(2.16)

Here g is the peak factor which represents the Gaussian process. This peak factor is derived by Davenport (1964) is widely used in wind engineering problems.

2.3 Non- Gaussian Probability Density Function

The probability density function applicable to the non-Gaussian random process was developed by applying the concept of polynomials orthogonal with

respect to the probability density function. The function of non-Gaussian process given in terms of standardized random data with mean m_x and the standard deviation σ_x , that is $x_0(t)=[x-m_x]/\sigma_x$ given by

$$P(x) = \varphi(x_0)\left[1 + \sum_{n=1}^{n} h_n H_n(x_0)\right] \qquad (2.17)$$

Where $\varphi(x_0)$ is the standard Gaussian probability density function, $\varphi(x_0) = (2\pi)^{1/2}\exp(-x_0^2/2)$ and the Hermite polynomials $H_n(x_0)$.

2.4 Gram- Charlier Probability Density Function

The Hermite polynomial of degree n, denoted by $H_n(x_0)$ is defined as a function which satisfies the following relationship given by

$$\frac{d^n}{dx_0}e^{-x_0^2/2} = (-1)^n H_n(x_0) \times e^{-x_0^2/2} \qquad n = 0,1,2,3......$$
$$(2.18)$$

From the above Equation, the following Hermite polynomials can be given as

$$H_0(x_0) = 1$$
$$H_1(x_0) = x_0$$
$$H_2(x_0) = x_0^2 - 1 \qquad (2.19)$$
$$H_3(x_0) = x_0^3 - 3x_0$$
$$H_4(x_0) = x_0^4 - 6x_0^2 + 3 \qquad etc$$

By applying the above Hermite polynomials the probability density function for the non-Gaussian processes derived by Ochi. (1986) and shown as

$$P(x) = \frac{1}{\sigma_x\sqrt{2\pi}}\exp\left(-\frac{1}{2}\frac{(x-m_x)^2}{\sigma_x}\right)$$
$$\times\left\{1 + \frac{\zeta_3}{3!}H_3\left(\frac{(x-m_x)}{\sigma_x}\right) + \frac{\zeta_4}{4!}H_4\left(\frac{(x-m_x)}{\sigma_x}\right)\right\}$$
$$(2.20)$$

Where, ζ_3, ζ_4 are the skewness and the kurtosis minus three of the distribution respectively. σ_x is the standard deviation. H3 and H4 are the respective hermite moments. Also, the Hermite moments of softening process ($\zeta_4 > 3$) are taken from Kareem *et al.* (2004)

2.5 Moment- Based Hermite Transformation Method

Hermite moment model represents the non-Gaussian random process in terms of Hermite polynomials considering the standard Gaussian process. Any non-Gaussian process x(t), can be expressed in terms of standard Gaussian process u(t) through a monotonic

function. Further, the relation between the standardized non-Gaussian and Gaussian for the softening process can be represented as follows,

$$x = \alpha\left\{u + h_3\left(u^2 - 1\right) + h_4\left(u^3 - 2u\right)\right\} \qquad (2.21)$$

Where,

$$\alpha = \left(1 + 2h_3^2 + 6h_4^2\right)^{-\frac{1}{2}} \quad h_3 = \frac{\zeta_3}{4 + 2\sqrt{1 + 1.5\zeta_4}}$$

and $\qquad h_4 = \frac{\sqrt{1 + 1.5\zeta_4} - 1}{18}$

Thus, by using this probability density function can be derived. Based on the studies, Grigoriu. (1984) and Winterstein. (1985), the crossing rate and the peak distribution can be derived by the Hermite moment method. The stationary mean crossing rate considering the skewness and kurtosis can be derived as

$$v(x) = v_{ng}\exp\left[-\frac{u^2(x)}{2}\right] \qquad (2.22)$$

$$v_g = \frac{1}{2\pi}\sqrt{\frac{m_2}{m_0}} \qquad (2.23)$$

Where $v_{ng} = \frac{1}{2\pi}\sqrt{\frac{m_2}{m_0}}\frac{1}{\alpha^2\left(1 + 4h_3^2 + 18h_2^2\right)}$ (2.24)

2.6 Non-Gaussian Peak Factor Formula

Kareem *et al.* (2004) shows the improved method for calculating the non-Gaussian peak factor by considering the skewness and kurtosis. The effect of the non-Gaussian terms such as skewness and kurtosis following the moment-based Hermite transformation approach.

In Poisson distribution model, the extreme value distribution for time period T is

$$P_{max}(x) = \exp\left\{-v_0 T\exp\left[-\frac{u^2(x)}{2}\right]\right\} \qquad (2.25)$$

Where $u(x)$ is the standardized Gaussian variable defined in the Eq. (2.2).The mean value of the positive maximum values over the time T can be given as

$$= \int_0^\infty x dP_{max}(x) = g.\sigma_x \qquad (2.26)$$

Where, g represents the peak factor and σ_x is the standard deviation of the random data x (t). For the Gaussian distribution and narrowband process Davenport. (1964) derived the expression shown in Eq. (2.16). It can be written as

Fig. 1(a). Experimental pressure model withonly tower case

Fig. 1(b). Experimental pressure model with tower and rotor case

$$g = \phi + \frac{\gamma}{\phi} \tag{2.27}$$

Where $\phi = \sqrt{\left(2 \log v_g T\right)}$, $\gamma = 0.5772$

In Kareem *et al*. (2004), the non-Gaussian peak factor for the narrowband approximation can be given as

$$g_{ng} = \mu \left\{ \begin{array}{l} \left(\phi + \dfrac{\gamma}{\phi}\right) + h_3\left(\phi^2 + 2\gamma - 1\right) + \\[2mm] h_4\left[\phi^3 + 3\phi(\gamma - 1) + \dfrac{3}{\phi}\left(\dfrac{\pi^2}{12} - \gamma + \dfrac{\gamma^2}{2}\right)\right] \end{array} \right\} \tag{2.28}$$

Where g_{ng} is the peak factor for non- Gaussian processes. Here, $\phi = \sqrt{\left(2 \log v_g T\right)}$, $\gamma = 0.5772$

3. EXPERIMENTAL SETUP

Boundary Layer open circuit Wind Tunnel with 18 m × 2.5 m × 2.15 m size test section with wind speed ranging from 0.5 to 55 m/s at Council of Scientific and Industrial Research – Structural Engineering Research Centre (CSIR-SERC) having the blockage ratio of less than 3 % is used for the present study. The wind speed can be simulated in a controlled fashion and various flow parameters can be calculated. The research centre is equipped with multi-channel pressure scanner which can measure simultaneous pressure measurement with the sampling frequency of 1000 Hz. The horizontal axis wind turbine pressure model with pressure taps for only tower and tower with rotor are shown in the Figs. 1(a) & 1(b) respectively for a scale ratio of 1:330.. Pressure taps made at every 30 deg at four

levels on wind turbine tower and the schematic of geometric details are shown in Figs. 2(a) – (b). There are totally 48 pressure points in the turbine tower distributed at the height of z/H = 0.2, 0.4, 0.6 and 0.8.

The turbulence intensity is less than 12% in the test section of the wind tunnel. Electronic pressure scanning is used to measure the pressure distribution on the surface of the tower and more than 10000 data per pressure point per set is obtained. Three nominal wind speeds were tested for the wind turbine configuration which corresponds to the Reynolds number ranging from $10^2 - 10^4$.

4. RESULTS AND DISCUSSIONS

In order to understand the probability distribution of the random pressure, probability density function is calculated and plotted for various pressure taps. Even though all the pressure tap data are analyzed for probability density function, certain pressure taps were considered for the discussion.

Probability distribution function for an example random pressure data in Fig. 3(a) for 10 seconds time period with a sampling frequency of 1000 Hz is shown in Fig. 3(b). The probability density function has been plotted initially for non– parametric fit and then compared with the corresponding Gaussian fit. As shown in Fig. 2(b) four levels of pressure have been measured where ports 1, 13, 25, 37 are facing towards the wind and can be considered as the stagnation point of the circular cylinder to that corresponding levels. Figures 4 (a), 5(a), 6(a) & 7(a) are the pressure taps located at the stagnation point which is the windward direction. Hence, the probability distribution of the non-parametric fit agrees with a Gaussian distribution. Figures 4(b), 5(b), 6(b) & 7(b) , 4(d), 5(d), 6(d) & 7(d) are the pressure taps on the sidewards of the wind turbine tower. The probability distribution function of the aforementioned ports deviates from the Gaussian
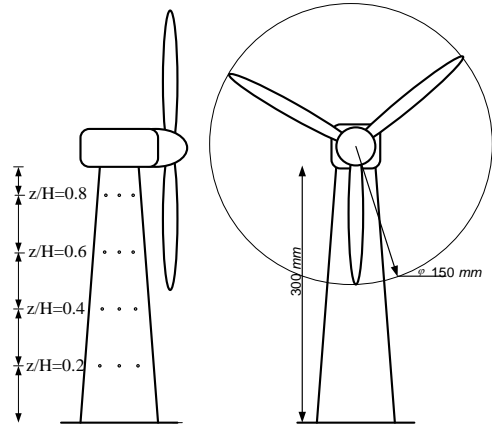
Fig. 2(a). Schematic of wind turbine model with pressure taps on various heights, Not to scale.
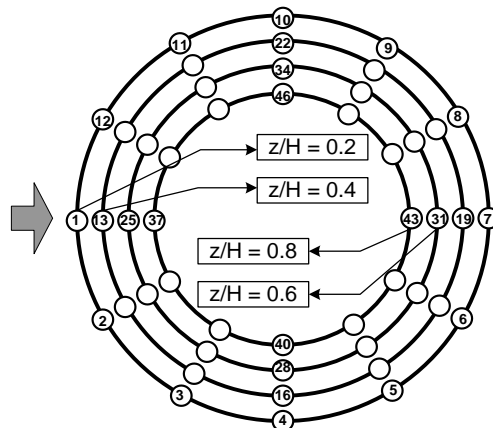

Fig. 2(b). Distribution of pressure taps on the surface of the tower at various height, Not to scale.
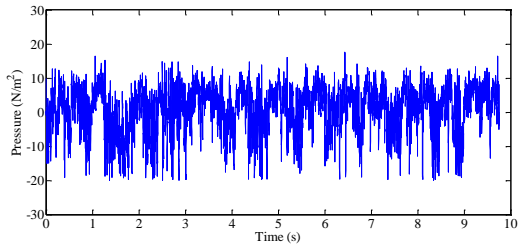

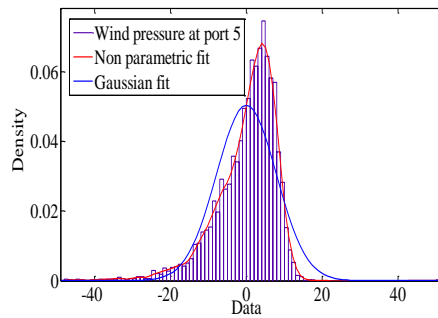**Fig. 3(a). Random pressure data measured from the wind tunnel for HAWT tower.**

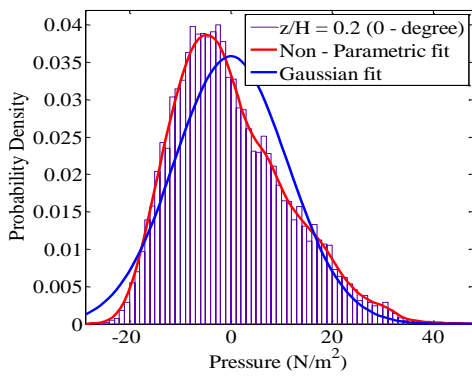**Fig. 3(b). Probability density function for an example random pressure data.**

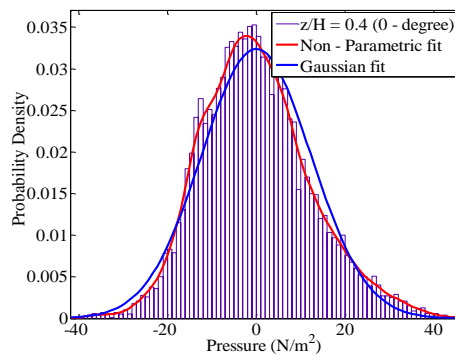**Fig. 4(a). Probability density at pressure tap 1.**
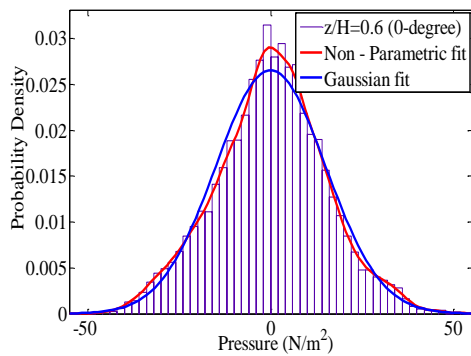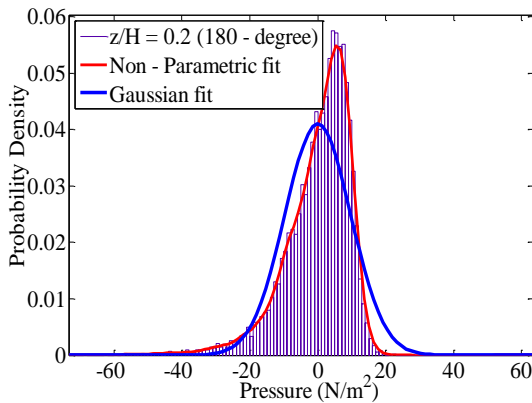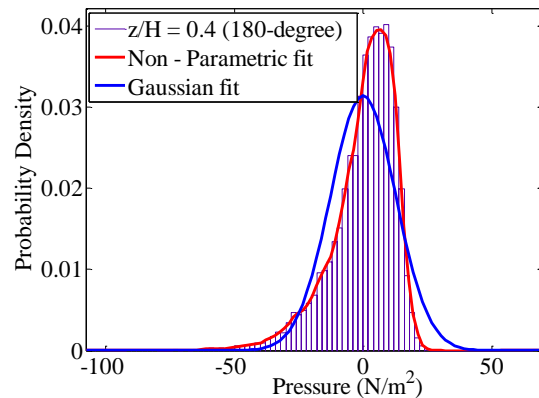

Fig. 4(b). Probability density at pressure tap 13.
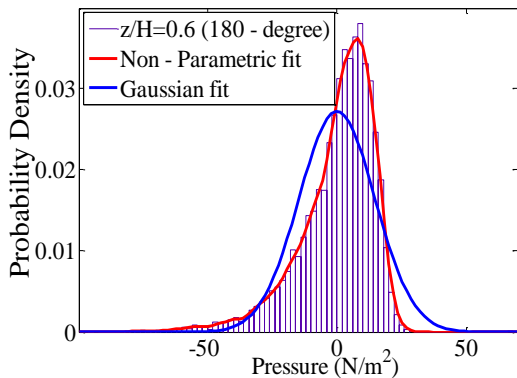

Fig. 4(c). Probability density at pressure tap 25.
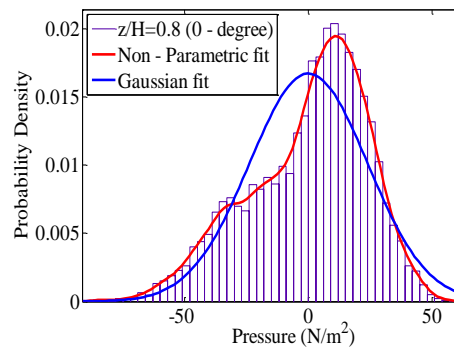
Fig. 4(d). Probability density at pressure tap 37.
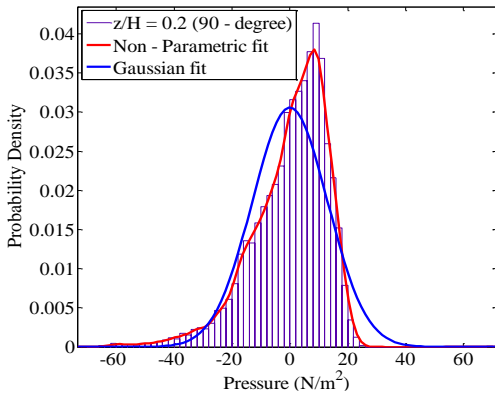
Fig. 5(a). Probability density at pressure tap 4.
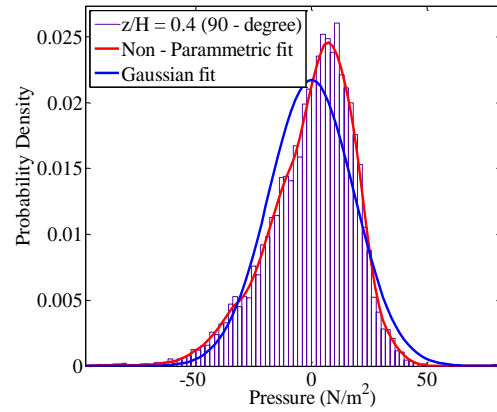
Fig. 5(b). Probability density at pressure tap 16.
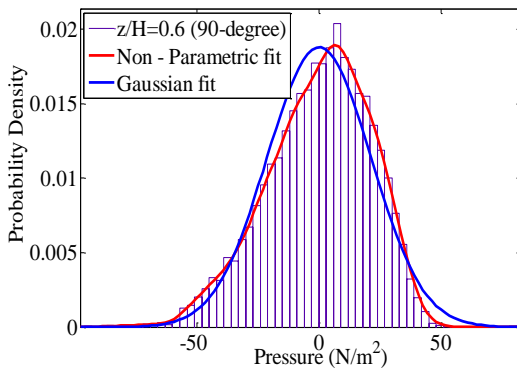
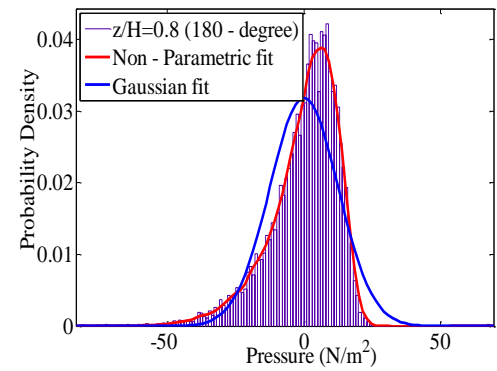**Fig. 5(c). Probability density at pressure tap 28.**
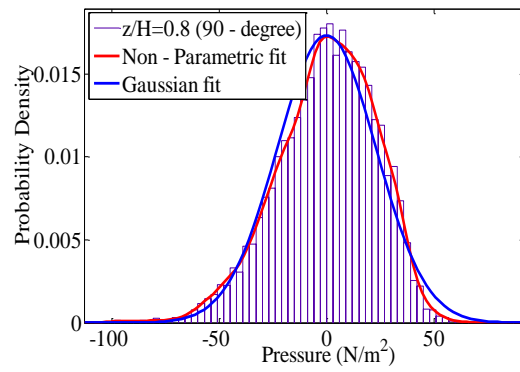
Fig. 5(d). Probability density at pressure tap 40.

Fig. 6(a). Probability density at pressure tap 7.

Fig. 6(b). Probability density at pressure tap 19.

Fig. 6(c). Probability density at pressure tap 31.

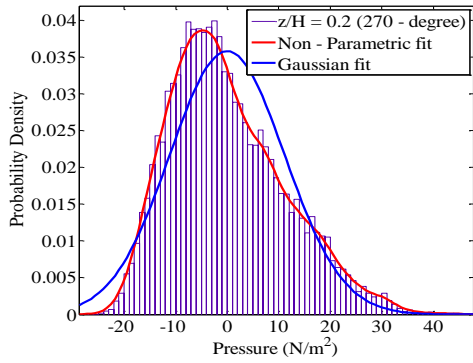**Fig. 6(d). Probability density at pressure tap 43.**

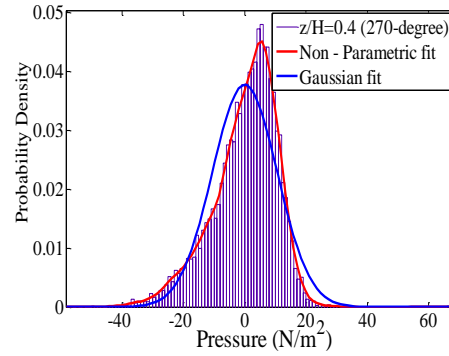**Fig. 7(a). Probability density at pressure tap 10.**

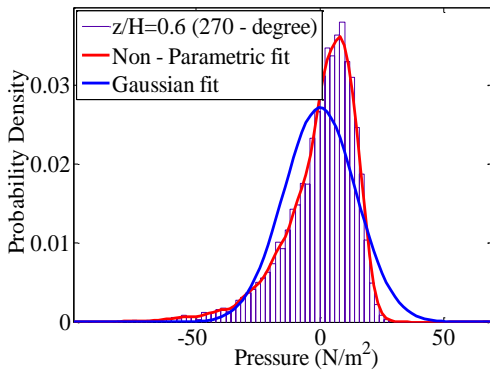**Fig. 7(b). Probability density at pressure tap 22.**
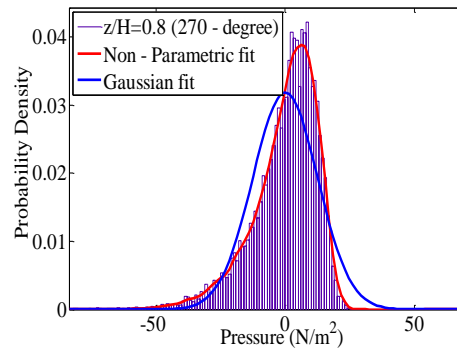

Fig. 7(c). Probability density at pressure tap 34.

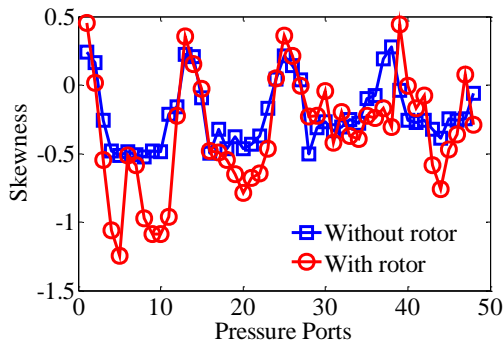**Fig. 7(d). Probability density at pressure tap 46.**

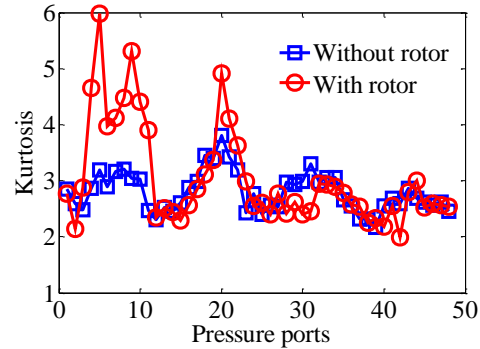**Fig. 8(a). Skewness for the pressure data with and without rotor rotation.**

Fig. 8(b). Kurtosis for the pressure data with and without rotor rotation.

fit. This is most likely due to the non-Gaussian behavior of random wind pressure data on the sideward ports. Figures 4(c), 5(c), 6(c) & 7(c) are the pressure taps on the leeward side of the wind turbine tower also deviates from the Gaussian fit and this may be due to the formation of wake region on the rear side of the wind turbine. Majority of the pressure distribution deviates from the Gaussian distribution where a mixed behavior, which is both Gaussian and non – Gaussian is widely seen from the skewness and kurtosis for the tower only and tower with rotor rotating cases shown in Figs. 8(a) & (b). In Fig. 8, the values shown at the lower levels are the cases where the influence of the rotor is insignificant, For example, the rotor rotation effect could be seen only in the levels z/H = 0.6 & 0.8. However, because of the rotor rotation, the influence is seen in z/H = 0.4 & 0.6. All these conditions are discussed for the

wind turbine when the rotor is rotating and tower only cases. Hence, the effect of non-gaussianity needs to be considered while designing the wind turbine tower. In order to understand the behavior of the non-Gaussianity, the peak factor analysis has been performed for the various pressure taps.

The characteristics of the non-Gaussian distribution function are generally represented by a third and the fourth moments which are skewness and kurtosis of the probability distribution function. The effect of non-gaussianity for the wind turbine tower with and without rotor has been shown in terms of skewness and kurtosis in Figs. 8(a) and 8(b) respectively. Figure 8(a) shows the characteristics where the skewness value is insignificant for even at tower only case. Hence, shows the symmetricity of the
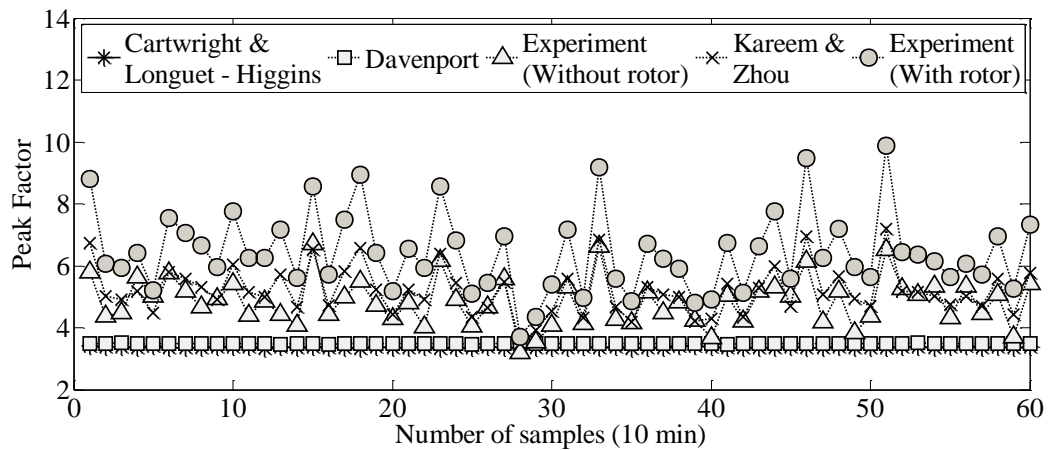
Fig. 9. Comparison of Theoretical and experimental peak factor on HAWT tower with and without rotor cases.

distribution for wind turbine without a rotor. However, for a wind turbine with rotor rotating shows considerable skewness value and proves the non-gaussianity at the lower levels where the influence of the rotating rotor is limited, By having such considerable skewness the peak factor cannot be predicted based on Gaussian assumption. Additionally, to compute the peak factor, it becomes quintessential to consider kurtosis values. Figure 8(b) shows kurtosis for both with and without rotor is considerable. Kurtosis value is predominant in the lower levels for the turbine with rotor case. Hence, the non-gaussianity of the random pressure data in HAWT tower needs a certain attention. Figure 9 shows the peak factor g based on the experimental data, Davenport, Kareem Zhou, Cartwright & longuet Higgins Peak factor for the Eq. (2.1). Further, it discerns that Davenport's method and Longuet – Higgins method doesn't exhibit significant difference, this may be because of the random process can be narrowband in the frequency domain. Davenport's method based on Eq. (2.16) which is based on Gaussian assumption couldn't predict the peak factor of the pressures on the surface of the HAWT. Also, Cartwright and Longuet – Higgins method underpredict the experimental peak factor. It is evident from Fig. 9 that Kareem Zhou's peak factor which is based on Hermit transformation agrees closely with the experimental results. This is because of Kareem Zhou peak factor method considers the non-gaussianity by including skewness and kurtosis. It can be seen from the results that the non-gaussianity in the random pressures dominates when the wind turbine with rotating rotor than the simple tower.

4. CONCLUSION

Wind turbine tower with various levels of pressure measured at different heights and the peak pressure is calculated and the following conclusions are made.

(i)   The pressure distribution follows the Gaussian distribution for the random pressure data of the HAWT tower and it can be evident from the skewness and kurtosis values.

(ii) The Davenport's method to calculate the maximum value is applicable for the HAWT without rotor and also the stagnation points of the tower with a rotor which is generally Gaussian nature.

(iii) For a HAWT tower with the rotor, considerable non-Gaussian behavior for the random pressure data has been observed which should be considered while designing the tower structure.

(iv) For such non-Gaussian behavior peak factor of the experimental random pressures agrees very well with Kareem Zhou's non-Gaussian peak factor method.

The wind turbine model is placed in a uniform wind speed test section limited to open terrain condition of atmospheric boundary layer terrain category. However, for peak value, non-Gaussian behavior needs to be considered while designing the HAWT tower systems.

REFERENCES

Cartwright, D. E. and M. S. Longuet-Higgins (1956). Statistical Distribution of the maxima of a random function. *Proc. Roy. Soc.A 237*, 212-232.

Ching-Wen C. and J. Jing-Jong (2009). *A Study of wind resistant safety design of wind turbines tower system.* (APCWE-VII), November 8-12, Taipei, Taiwan

Davenport, A. G. (1964). Note on the distribution of the largest value of a random function with application to gust loading. *Proceedings, Institution of Civil Engineers 28,* 187-196.

Dimopoulos, C. A. and C. J. Gantes (2012). Experimental investigation of buckling of wind turbine tower cylindrical shells with opening and stiffening under bending, *Thin-Walled Structures 54*, 140-155.

Global Wind Report. (2014). Annual market update 2014, Global Wind Energy council.

Grigoroiu, M. (1984). Crossing of non-Gaussian translation processes. *Journal of Engineering Mechanics* 110(4), 610-620.

Gurley, K. R., M. A. Tognarelli and A. Kareem. (1997). Analysis and Simulation Tools for Wind Engineering *Probabilistic Engineering Mechanics 12,* 9-31.

Gusella, V. and A. L. Materazzi (2000). Non-Gaussian along-wind response analysis in time and frequency domains. *Engineering Structures 22*(1), 49-57.

Kareem, A. and J. Zhao (2004). Analysis of Non-Gaussian surge response of tension leg platforms under wind loads. *Journal of offshore mechanics and Artic Engineering 116*, 137-144.

Kwon D. K.., A. Kareem and K. Butler. (2012). Gust-front loading effects on wind turbine tower systems. *J. Wind Eng. Ind. Aerodyn 104-106*, 109 – 115.

Lavassas, I., G. Nikolaidis, E. Zervas, I. N. Efthimiou, C. C. Doudoumis and Baniotopoulos. (2003). Analysis and design of the prototype of a steel 1-MW wind turbine tower. *Engineering Structures 25*(8), 1097-1106.

Luong Van Binh., Takeshi Ishihara., Pham Van Phuc., & Yozo Fujino. (2008). A peak factor for non-Gaussian response analysis of wind turbine tower. *Journal of Wind Engineering and Industrial Aerodynamics 96*(10–11), 2217-2227.

Nadaraja Pillai, S. and Y. Tamura (2009). Generalized peak factor and its application to stationary random processes in wind engineering applications. *Journal of wind and Engineering 6*(1), 1-10.

Noda, H., K. Shimada and T.Ishihara. (2005). *Wind Forces and Peak Wind Pressure Distributions on Wind Turbine Nacelle*. (APCWE-VI), Seoul, South Korea.

Ochi, M. K. (1986). Non-Gaussian random processes in ocean engineering. *Probabilistic Engineering mechanics 1*(1), 28-39.

Tamura, Y. (2009). *Wind induced damage to buildings and disaster risk reduction*. (APCWE-VII), Taipei, Taiwan.

Winterstein, S. (1985). Non-normal responses and fatigue damages. *Journal of Engineering Mechanics. 111*(10), 1291-1295.